Neuron, Vol. 37, 977–987, March 27, 2003, Copyright ©2003 by Cell Press

Arithmetic of Subthreshold Synaptic Summation in a Model CA1 Pyramidal Cell

Panayiota Poirazi,[1,*] Terrence Brannon,[2] and Bartlett W. Mel[3,*]
[1]Institute of Molecular Biology and Biotechnology
Foundation for Research and
Technology, Hellas (FO.R.T.H.)
Vassilica Vouton
P.O. Box 1527
GR 711 10 Heraklion, Crete
Greece
[2]Metaperl IT Consulting
135 Corson Avenue
Staten Island, New York 10301
[3]Department of Biomedical Engineering and
Neuroscience Graduate Program
University of Southern California
Los Angeles, California 90089

Summary

The rules of synaptic integration in pyramidal cells remain obscure, in part due to conflicting interpretations of existing experimental data. To clarify issues, we developed a CA1 pyramidal cell model calibrated with a broad spectrum of in vitro data. Using simultaneous dendritic and somatic recordings and combining results for two different response measures (peak versus mean EPSP), two different stimulus formats (single shock versus 50 Hz trains), and two different spatial integration conditions (within versus between-branch summation), we found that the cell's subthreshold responses to paired inputs are best described as a sum of nonlinear subunit responses, where the subunits correspond to different dendritic branches. In addition to suggesting a new type of experiment and providing testable predictions, our model shows how conclusions regarding synaptic arithmetic can be influenced by an array of seemingly innocuous experimental design choices.

Introduction

Pyramidal cell dendrites are known to contain an elaborate mixture of voltage-dependent currents, which contribute to complex active responses, including fast and slow dendritic spikes confined to the dendrites and various subthreshold modulatory effects (Magee et al., 1998; Häusser et al., 2000; Reyes, 2001). Many questions remain, however, regarding the contributions of these highly nonlinear membrane mechanisms to synaptic integration. Based on principles of biophysics and cable theory, a dendritic spike-generating mechanism would seem likely to produce strong superlinear interactions among nearby excitatory inputs. For example, a doubling of synaptic excitation should lead to a more than doubling of the voltage response if a local dendritic spike threshold is crossed.

*Correspondence: poirazi@imbb.forth.gr (P.P.), mel@usc.edu (B.W.M.)

Superlinear summation of synaptic inputs has indeed been observed in pyramidal (Schwindt and Crill, 1998; Margulis and Tang, 1998; Nettleton and Spain, 2000) and other cells (Wessel et al., 1999). In addition, synaptically evoked NMDA spikes confined to individual dendritic branches (Schiller et al., 2000; Wei et al., 2001; K. Holthoff, D. Tsay, and R. Yuste, R, 2000, Soc. Neurosci., abstract) and boosting effects mediated by Na^+ and/or Ca^{2+} channels (Lipowsky et al., 1996; Gillessen and Alzheimer, 1997; Gonzalez-Burgos and Barrionuevo, 2001) suggest that a strong superlinearity should under some conditions be evident in the conversion of synaptic input to somatic responses. Seemingly at odds with this, Cash and Yuste (1999) reported that in CA1 pyramidal cells, summation of EPSPs driven by glutamate iontophoresis onto different parts of the same dendrite was sublinear in the apical trunk and "overwhelmingly linear" elsewhere (see also Skydsgaard and Hounsgaard, 1994; Cash and Yuste, 1998; Urban and Barrionuevo, 1998; A.D. Reyes and B. Sakmann, 1996, Soc. Neurosci., abstract).

Are these differences real, or might they arise in part from subtle differences in experimental design? If r denotes response and A and B are two discrete stimuli, the hypothesis tested by a typical pairwise summation experiment can be expressed schematically as follows:

$$r(A + B) = r(A) + r(B), \quad (1)$$

where satisfaction of Equation 1 corresponds to linear summation. One difficulty in interpreting the results of such studies stems from the choice of stimulus format and response measure. For example, in vitro studies of synaptic integration in pyramidal cells have usually involved summation of discrete EPSPs or EPSP-like waveforms and have often used somatic EPSP peak height to quantify summation (Urban and Barrionuevo, 1998; Margulis and Tang, 1998; Cash and Yuste, 1999). This measure emphasizes the first few milliseconds of the response, leaving open the possibility that a measure emphasizing the late response or the totality of the response, such as the EPSP half-width, area, or mean (e.g., Wessel et al., 1999; Nettleton and Spain, 2000), might produce different results. Moreover, in dendrites containing active channels with slow kinetics, such as NMDA-type synaptic conductances and voltage-dependent Ca^{2+} channels, or slowly inactivating K^+ channels, the response to a single large, synchronous EPSP-like event produced by an extracellular shock or glutamate pulse is not necessarily a reliable predictor of the neuron's response to high-frequency synaptic inputs applied for longer times. This latter concern is bolstered by the observation that calcium spikes often emerge in dendritic recordings only in response to sustained input (Golding et al., 1999) and by the observed gradual shift from sublinear to superlinear temporal summation in CA1 pyramidal cells during stimulus trains (Cash and Yuste, 1999).

Another difficulty in interpreting the results of pairwise summation experiments arises from a combination of

poor stimulus control and poor visibility of distal integrative events. The use of glutamate iontophoresis or laser uncaging or direct electrical stimulation of presynaptic fibers usually means incomplete knowledge or control of the number, exact whereabouts, or subtype of channel activated (i.e., AMPA versus NMDA, ionotropic versus metabotropic). This uncertainty, coupled with the poor visibility of distal electrical responses provided by a single somatic recording electrode, could lead to the delivery of stimuli which are too weak, too strong, or too restricted in range to properly characterize the nonlinear interactions among synapses which may occur in the distal dendrites.

This problem may be highlighted by contrasting the predictions of two different models of subthreshold dendritic integration, one linear and one nonlinear, both of which can be expressed by a single equation

$$r = \sum_{i=1}^{m} \alpha_i s(x_i) \quad (2)$$

where x_i is the total input to the ith dendritic subunit, s is the subunit input-output function, α_i is the subunit's weight, and m is the number of subunits. In the special case where $s(x) = x$, Equation 2 reduces to cell-wide linear summation

$$r = \sum_{i=1}^{m} \alpha_i x_i \quad (3)$$

which corresponds to the classical linear "point neuron" hypothesis. In this case, it is clear that Equation 1 will be satisfied for stimuli of all magnitudes, for stimulus pairs that are balanced [$r(A) \approx r(B)$] or unbalanced [$r(A) >> r(B)$], and when A and B are delivered to the same or different dendritic subunits. In one instance, Cash and Yuste (1999) contrasted within-branch and between-branch summation in the basal dendrites of CA1 pyramidal cells. However, the experiment was carried out in the presence of NMDA and Na^+ channel blockers, making it difficult to extrapolate to the integrative behavior of an intact cell.

In contrast, when the subunit function $s(x)$ is nonlinear, Equation 2 becomes a bona fide two-layer nonlinear model. For example, assuming $s(x) = sigmoid(x)$, the nonlinear model predicts that for balanced stimuli delivered to a single subunit, (1) very weak inputs will sum nearly linearly, (2) intermediate inputs that produce threshold crossings will sum superlinearly, and (3) very strong inputs will sum sublinearly. Furthermore, unbalanced inputs will produce near-linear summation over the entire range of stimulus intensities, and when inputs are delivered to two different subunits, summation will also be linear for all stimulus combinations and strengths.

Our goal has been to (1) assess how well the linear versus nonlinear models of synaptic integration account for the arithmetic of summation in CA1 pyramidal cells and (2) identify those aspects of experimental design that may have contributed to conflicting interpretations of existing experimental data. To do this, we developed a biophysically detailed compartmental model of a CA1 pyramidal cell, allowing us to precisely control the number, location, and character of the stimulated synapses and to record the postsynaptic response at all locations within the cell simultaneously (see the Supplemental Data available online at http://www.neuron.org/cgi/content/full/37/6/977/DC1 for a full description of the model). We focus on summation within the synapse-rich thin terminal branches of the apical tree and run several variants of $A + B$ synaptic summation experiments to compare the predictions of the two different models of synaptic arithmetic. In particular, we

- explore the entire range of stimulus intensities and levels of balance and explicitly track the results for each identified dendritic subunit,
- compare results for two different subthreshold response measures that emphasize different time courses of the response,
- compare results for two different stimulus formats, including discrete single-pulse stimuli and high-frequency trains, and
- compare results for within-branch versus between-branch summation.

The results of each of our new simulation experiments lead to predictions that can be tested experimentally using currently available methods. In a companion paper in this issue of *Neuron* (Poirazi et al., 2003), we extend our investigation to the suprathreshold case in which many subunits are driven simultaneously with high-frequency inputs, and somatic responses are quantified by spike rate.

Results

The compartmental model used in this work was run within the NEURON simulation environment (Hines and Carnevale, 1997) using the reconstructed CA1 pyramidal neuron shown in Figure S1 of the Supplemental Data available online at http://www.neuron.org/cgi/content/full/37/6/977/DC1. The cell morphology was obtained from the Duke/Southampton archive (Cannon et al., 1998). The biophysical model consists of 183 compartments and includes a variety of passive and active membrane mechanisms known to be present in CA1 pyramidal cells. These include a leak current (I_{leak}), two kinds of Hodgkin-Huxley-type sodium and potassium currents (somatic/axonic I^{sa}_{Na} and I^{sa}_{Kdr}, dendritic I^{d}_{Na} and I^{d}_{Kdr}), two types of A-type (proximal and distal) and one of m-type potassium currents (I^{p}_{A}, I^{d}_{A}, I_m), a mixed conductance hyperpolarization-activated h-current (I_h), three types of voltage-dependent calcium currents, namely, a LVA T-type current (I_{CaT}), two HVA R-type currents (somatic, I^{s}_{CaR}; dendritic, I^{d}_{CaR}), and two HVA L-type currents (somatic, I^{s}_{CaL}; dendritic, I^{d}_{CaL}), two types of Ca^{2+}-dependent potassium currents (a slow AHP current, I^{s}_{AHP}; and a medium AHP current, I^{m}_{AHP}), a persistent sodium current (I^{p}_{Na}), and four types of synaptic currents, namely, AMPA, NMDA, $GABA_A$, and $GABA_B$. Densities and distributions of the mechanisms included in our model are based on published empirical data and are fully described in the Supplemental Data at http://www.neuron.org/cgi/content/full/37/6/977/DC1.

The validation studies shown in Figures S1 and S2 of the Supplemental Data (http://www.neuron.org/cgi/content/full/37/6/977/DC1) show that the model exhibits (1) several I_h-dependent effects, including a realistic sag current, reasonable values for input resistance in the soma and dendrites, and the characteristic pattern of

asymmetric voltage attenuation traveling to and from the cell body through the apical trunk; (2) a realistic pattern of distance and time-dependent attenuation in trains of back-propagating action potentials, with appropriate dependence on I_A; and (3) the elicitation of delayed-onset Ca^{2+} spikes from a distal but not proximal stimulating electrode.

Linear versus Nonlinear Summation of EPSPs

Following the logic of Equation 1, studies of synaptic integration have most often involved a comparison of the somatic EPSP in response to a combined stimulus to the prediction consisting of the sum of the responses to the individual stimuli. Depending on whether the actual combined response exceeds, equals, or falls short of the prediction, synaptic integration is dubbed superlinear, linear, or sublinear, respectively.

In a systematic study of synaptic integration in CA1 pyramidal cells, Cash and Yuste (1999) found that summation was sublinear for stimuli delivered to two different locations along the apical trunk, especially for larger combined responses (Figure 1A). Using pharmacological blockers for NMDA channels, Na^+ channels, Ca^{2+} channels, and A-type K^+ channels, they found that the nonlinear suppression of combined responses was due primarily to voltage-dependent rectification by I_A, which is present in high concentrations in the apical tree (Figure 1B). Urban et al. (1998) reported a similar finding in CA3 pyramidal cells and interpreted the A-current as contributing to an active linearization of synaptic integration.

We tested our model cell in the same way, with synaptic stimuli delivered separately and together to two randomly drawn sections of the apical trunk. On each section, a randomly drawn number between 2 and 12 excitatory synapses separated by 2 μm was activated synchronously, and the peak of the resulting EPSP was recorded at the cell body. Individual responses below 1mV were rejected, as were responses that produced a somatic spike. Synaptic conductances were scaled locally in this and all other experiments so that a single EPSP gave a peak 5mV depolarization at the site of the synapse. This scaling was not intended to model the actual elemental synaptic conductance value, which may in fact vary with dendritic location (Magee and Cook, 2000), and had no impact on the form of the results (whether linear, sublinear, etc.) but simplified automatic generation of a large number of experiments covering a reasonable range of postsynaptic potentials.

The response to the synchronous activation of both sets of synapses was recorded, and the trial was again rejected if a somatic spike occurred. For each valid trial, we plotted the expected EPSP peak on the *x* axis and the actual EPSP peak on the *y* axis (Figure 1C), showing a sublinear trend similar to that reported by Cash and Yuste (1999); open squares denote five corresponding fiducial points to facilitate comparison of the two graphs. A set of pseudopharmacological manipulations was also carried out comparable to those of the Cash and Yuste study, yielding a similar pattern of results (Figure 1D). In one difference, our cell did not yield subthreshold combined responses as large as the cells reported in Cash and Yuste (1999), topping out at 10mV rather than 20mV. This could be explained in part by the greater role played by Na^+ currents in the apical trunk of our model cell, as evidenced by the slightly taller control column and slightly shorter Na^+-block column in Figure 1D versus 1B. This excess of Na^+ channel activity could explain our inability to generate very large (e.g., >15mV) depolarizations at the soma that failed to trigger somatic spikes. Nevertheless, over the range of data acquired, model responses were closely matched to the experimental data.

We repeated the experiment using a pair of stimuli delivered separately and together to a terminal oblique section or a terminal branch in the apical tuft; a total of 38 branches were included in the set. In this case, synapses for the two stimuli were uniformly distributed along the length of the branch and physically interdigitated. Results from the Cash and Yuste (1999) study are shown in Figures 2A and 2B, and those from the model cell are shown in Figures 2C and 2D. The average percent of linearity for summation of EPSPs within the thin branches was just above the linear benchmark. Our slightly higher average value (107% in the model cell versus 101% in Cash and Yuste [1999]) is partly attributed to our lack of very large expected response cases in the range of 14mV to 18mV, which in the Cash and Yuste data set were strictly sublinear (Figure 2A). In addition, the model cell exhibited slightly less Na^+- and Ca^{2+}-dependent excitability in the thin branches compared to Cash and Yuste, judging by the reduced effect of sodium and calcium current blockade in the model cell (Figure 2D). Overall, however, the composite pattern of scatter data representing summation of EPSP peaks within the thin branches, and the dependence of summation on NMDA, Na^+, and Ca^{2+} currents, was similar to the experimental data of Cash and Yuste (1999).

Effect of Recording Site and Summation Measure

To provide a fuller view of the data, we repeated the thin-branch EPSP summation experiments, plotting both peak and mean response measures for a dendritic (Figure 3A) and somatic (Figure 3B) recording site. Red symbols loosely clustered along the diagonal in Figure 3B correspond to the within-branch stimulation data of Figure 2C for a single thin oblique branch 232 μm from the soma. The three other data sets in Figures 3A and 3B represent different measurements taken during the same set of experiments. Red symbols in Figure 3A show summation of EPSP peaks from the perspective of a dendritic electrode placed directly in the thin branch receiving the synaptic input. Horizontal light gray lines link each set of experiments with a fixed total number of synapses in the combined condition, explaining the identical actual depolarization values in each case (i.e., only the predictions differ). Circles connected by red lines indicate balanced cases (e.g., 4 + 4 synapses); squares clustered along the diagonal represent maximally unbalanced cases ($2 + n$ synapses for $1 < n < 28$). Triangles show the most superlinear (leftmost) and most sublinear (rightmost) case within each horizontal group, unless such cases were already indicated by a circle or square. Intermediate cases were omitted for clarity.

At an expected value of around 20mV for the com-

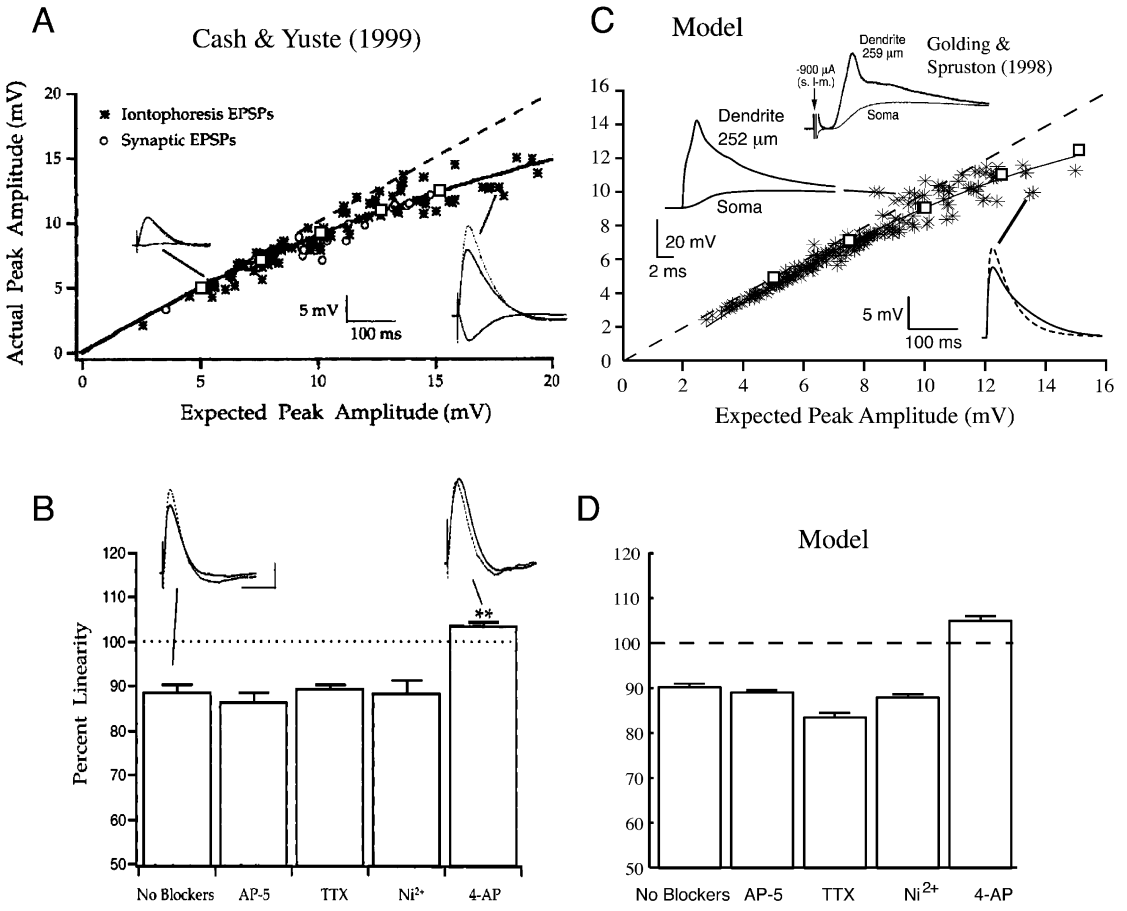

Figure 1. Summation of EPSP Peaks in Apical Trunk

(A) Excitation was delivered to two trunk locations beyond 100 μm, first individually and then synchronously. Peak of the combined EPSP (*y* axis) was plotted against expected response, given by the sum of individual somatic EPSP peaks (*x* axis). Data reproduced with permission from Cash and Yuste (1999) shows sublinear summation in apical trunk. Inset shows expected (dotted) versus actual (solid) traces for two cases. Open squares were added to facilitate comparison to model responses in (C).

(B) Blockade of NMDA (AP-5), Na^+ (TTX), or Ca^{2+} (Ni^{2+}) currents shows relatively small effect on sublinearity in the somatic response, while blockade of I_A (4-AP) leads to large upswing in percent linearity.

(C) Model responses to be compared with data in (A). Inset shows isolated dendritic spike accounting for superlinearity in a cluster of cases in the 10mV range. A comparable trace is reproduced from Golding and Spruston (1998).

(D) Effects of channel blockade in model cell are similar to experimental data shown in (B).

bined response, corresponding roughly to the local Na^+ spiking threshold in our model, the dendritic response to six total synapses jumps far above the linear prediction. For example, a 25mV expectation in the balanced case of $A = B = 4$ synapses leads to a 50mV actual response. Then, given that the response peak is largely determined by the local Na^+ current, which is essentially all-or-none in character, the actual response becomes nearly flat as inputs grow larger. For expectations in excess of 50mV, the negligible growth of actual responses pushes the data below the diagonal into the sublinear range. The inset shows actual (solid) versus predicted (dashed) voltage traces for one stimulus pair, indicated by four asterisks in Figures 3A and 3B.

The clear progression from linear to superlinear to sublinear summation at the dendritic recording site for weak, intermediate, and strong balanced stimuli is indicative of the powerful thresholding nonlinearity provided by the local dendritic spike-generating mechanism. This highly nonlinear pattern of summation for EPSP peaks is much less evident when EPSP peaks are measured at the soma (red symbols in Figure 3B). The superlinear range for six to ten synapses remains in evidence but appears in the very low response range under 4mV in comparison to the 40mV to 60mV generated distally. At the other end of the response continuum, the huge local sublinearity arising from summation of the two very strong inputs is also markedly attenuated at the soma. For comparison, the largest upward and downward deviations from the main diagonal at the distal electrode are +23mV (eight synapses) and −48.6mV (28 synapses), respectively, while at the soma the maximum deviations seen for these same synapse totals are +1mV and −1.32mV. The maximum deviations at the soma reached +3.38mV and −1.32mV over all cases. These min and max deviation cases at the soma are shown connected with dashed lines in Figure 3B and are reproduced in Figure 3C along with the comparable min and

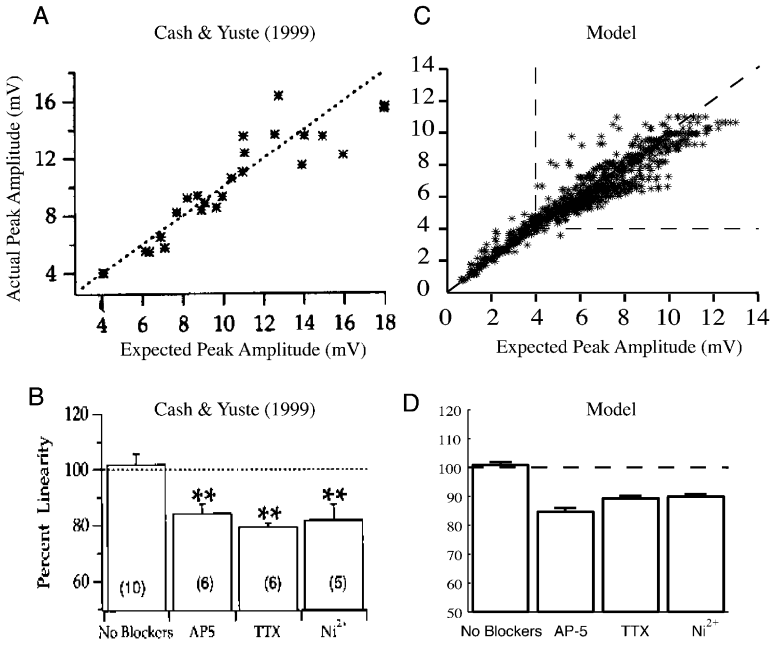

Figure 2. Summation of EPSP Peaks in Thin Apical Dendrites

(A) Data reproduced with permission from Cash and Yuste (1999) shows that summation of two inputs to a thin branch appears linear. (B) Same manipulations as in Figure 1B show much greater role for NMDA, Na^+, and Ca^{2+} currents in side branches compared to trunk. (C) Thin-branch summation scatter plot. Individual stimuli took on all magnitudes between 2 and 28 synapses incrementing by twos, to create combined stimuli ranging from 4 to 30 synapses. Summation results from model cell roughly straddle diagonal of linearity, as in (A). Dashed coordinate axes indicate origin of Cash and Yuste data to simplify comparison. (D) Changes in summation behavior under same channel-block conditions as in (B).

max deviations for 19 other thin branches in the apical tree. The compression of the deviations at the soma compared to the dendritic recording site is due primarily to the attenuation of fast spike responses in the course of their travel from a thin distal branch into the main trunk and on to the cell body.

When the mean (time-averaged) EPSP was used as a response measure rather than the EPSP peak, the pattern of summation was altered. First, given the much slower time course of the mean response, we found that summation arithmetic was more similar at the dendritic and somatic recording sites than was the case for peak responses (blue symbols in Figures 3A and 3B). Second, virtually all summation of mean responses was in the linear to superlinear range at both recording sites. Third, whereas the maximum superlinearity was observed at the low end of the peak response range, the maximum superlinearity for summation of mean responses was found at the high end of the response range (see connected min-max pair in Figure 3B, reproduced in Figure 3D). Fourth, by comparing peak and mean responses recorded at the two sites during the same experiment, it was possible to dissociate the pattern of summation for the two response measures. As shown by the insets and asterisks in Figures 3A and 3B (10 + 16 synapses), summation at the soma was marginally sublinear for EPSP peaks (−1%) and superlinear for EPSP means (+34.4%), with a similar but exaggerated dichotomy at the dendritic recording site.

Summation of EPSPs in Same versus Trunk-Separated Tips

It is clear from the results of Figures 3A and 3B that voltage-dependent interactions between two inputs delivered to a thin branch in the apical tree lead to significant deviations from the linear prediction when measured either in the dendrites or at the cell body. However, these experiments do not prove that the observed nonlinear interaction occurs locally within the stimulated branch. The interaction could be due to a single dendrite-wide or cell-wide nonlinearity triggered by inputs to a single branch. To address this question, we compared within-branch summation to between-branch summation for 20 thin branches in the apical tree drawn at random from the complete set of 38.

The results are shown in Figures 3C and 3D. For the within-branch data, the most sublinear and most superlinear cases were culled out for each of the 20 branches and were used to represent that branch's "envelope" of nonlinear summation. For summation of EPSP peaks, the 20 min-max pairs are shown as red triangles connected by lines in Figure 3C. This provided a sparser and more usefully annotated view of the cloud of scatter data shown in Figure 2C. For summation of EPSP means, the min-max pairs are shown as blue crosses connected by lines in Figure 3D. As can be seen in the population of combined peak and mean summation results for the 20 branches, the single branch described in detail in Figures 3A and 3B showed only modest deviations from linearity in comparison to many other branches tested.

To complete the picture, we repeated the same set of summation experiments but with stimuli delivered to two *different* terminal oblique or tuft branches separated by the apical trunk. Two sister branches on the same thin-branch subtree were excluded. Branch pairs were drawn at random from the same 38 terminal sections as before. The results of these experiments are shown as green circles in Figures 3C and 3D. All recordings were made at the cell body. In the case of EPSP peaks, the between-branch summation data are tightly clustered along the main diagonal (green circles in Figure 3C) and lie almost entirely inside the envelopes of the within-branch summation data. Thus, when EPSP peaks were measured, summation of inputs delivered to two different branches was close to linear for all branches,

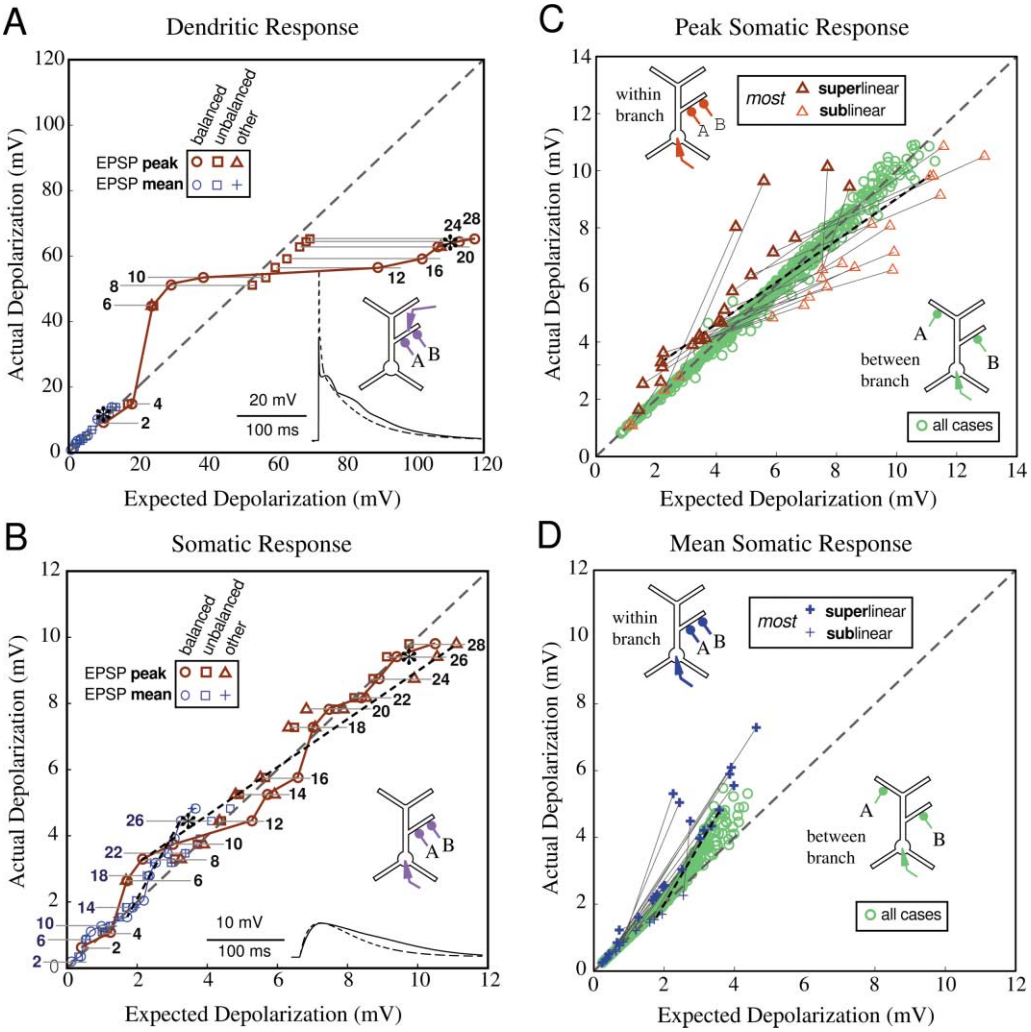

Figure 3. Effects of Recording Site, EPSP Response Measure, and Stimulus Configuration on Summation in Thin Branches of Apical Tree

(A) Repetition of within-branch stimulation experiment of Figure 2C but for responses measured within the stimulated dendritic branch. Results are shown for both peak (red) and mean EPSP (blue) in a single terminal branch connected to the apical trunk 232 μm from the soma. Annotated horizontal groupings of data represent cases with identical total number of synapses in the combined stimulus. Only leftmost and rightmost data points are shown in each group (triangles), along with balanced (circles) and unbalanced cases (squares). Balanced cases are connected by solid lines. Inset shows expected versus actual traces for one experiment with A = 10 and B = 16 synapses; results for this case are marked by four asterisks in (A) and (B).

(B) View of the same data set from somatic recording electrode. Dashed lines connect most superlinear and most sublinear cases for both peak and mean response measures. Lines threading balanced cases correspond exactly to the same in (A), as do unbalanced cases in each horizontal data group.

(C) Comparison of within-branch versus between-branch summation for EPSP peaks measured at the soma. Within-branch data for 20 branches are represented by a connected pair of extrema values; dashed line corresponds to the same in (B). Between-branch data include all cases tested.

(D) Same as (C) but showing summation of EPSP mean values at soma.

for all stimulus intensities, and for all degrees of stimulus balance. For summation of EPSP means, the between-branch summation data were also more tightly clustered and more linear than the within-branch data (Figure 3D). For very strong inputs, however, a significant upward bend was observed in the between-branch data, indicating a nonlinear boosting interaction between the two stimulated branches. We found that this branch-to-branch interaction depended on slow-acting dendritic calcium channels (data not shown) and was only clearly present when (1) the cell was stimulated with a single very strong synchronous input pulse and (2) summation was assessed using a slow (i.e., time-averaged) response measure. The trend was not seen, for example, when EPSP peaks were measured (Figure 3C).

Overall, the data shown in Figure 3 support a clear rejection of the linear summation hypothesis, since summation within virtually every one of the 20 branches tested showed a predictable pattern of significant deviations from linearity. For any given branch, the most superlinear peak response averaged 130% relative to the linear benchmark, and the most sublinear response av-

eraged 83%. For mean responses, the most superlinear and sublinear summation on a branch averaged 138% and 99%, respectively. By comparison, for any given *pair* of branches in the between-branch experiments, the most superlinear and sublinear responses for the pair averaged 104% and 94% for EPSP peaks, and 121% and 101% for EPSP means. Clearly in this model synapses interact more nonlinearly when they lie on the same branch than when they lie on different branches, which is the heart of the sum-of-subunits hypothesis expressed by Equation 2.

Less clear is the precise form of the nonlinear interaction, that is, the form of a dendritic subunits input-output function. Based on dendritic recordings of EPSP peaks, a sigmoidal nonlinearity is suggested by the clean progression from linear to superlinear back to linear and then sublinear summation for balanced inputs (Figure 3A, red symbols). At the somatic recording electrode, however, summation appears to be governed by a more complex bi-lobed function for both peak and mean response measures (Figure 3B). A second complication arises from the finding of a significant slow boosting interaction when strong inputs are delivered to two different branches (Figure 3D). Such an interaction cannot be accommodated by the simple functional form of Equation 2, which holds that the two subunit outputs should combine linearly.

Either of these complexities could signal that the sum-of-sigmoid-subunits model is inadequate to predict the summation of paired inputs in this very complex model cell. Another possibility is that the complexities are artifactual and arise from our use of a highly unnatural stimulus. A subthreshold EPSP-like response, evoked by a single discrete impulse delivered synchronously to a population of excitatory synapses on a resting cell, provides a simple and convenient measure of synaptic action. However, such a stimulus represents a radical simplification of the stimulus conditions that are likely to exist in vivo. Under natural conditions, a neuron is likely to receive trains of synaptic input that involve both excitatory and inhibitory pathways acting over considerably longer times. For this reason, we set out to assess the arithmetic of pairwise summation under more realistic stimulus conditions.

Summation of Trains in Same versus Trunk-Separated Tips

We repeated the experiments of Figure 3 using 50 Hz random trains lasting 250 ms. Given the much greater intensity of the stimulus in this case, inhibitory synapses were included to prevent the cell from entering an uncontrolled epileptic-like state. Specifically, each individual stimulus consisting of one or more excitatory synapses was accompanied by one inhibitory synapse activated at the center of the branch. The inhibitory synapse was also activated at 50 Hz and contained both a $GABA_A$ and $GABA_B$ conductance.

Summation results for the 50 Hz stimulation case are shown in Figure 4. The pattern of scatter data was similar to that of the discrete impulse case, with a few differences. First, we again found clear evidence for a sigmoidal subunit nonlinearity at the distal recording electrode. However in comparison to single-shock stimulation, peak and mean response measures gave results that were more similar to each other both in magnitude and in form at both recording electrodes. This was to be expected since the 250 ms stimulus duration meant peak and mean response measures were now *both* slow, in the sense that the peak was now extracted from a trace of much longer duration and potentially containing multiple peaks. Second, a sigmoidal summation nonlinearity was now clearly present at the soma for both peak and mean response measures (Figure 4B). Thus, unlike the single-shock case, the dendritic and somatic recording electrodes in this case tell a very similar story (compare Figures 4A and 4B). Third, within-branch summation was now dominated by data in the linear to superlinear range for both response measures (Figure 4). This was due to the fact that inputs strong enough to drive the dendritic compartment deep into the sublinear range generally also triggered somatic spikes. Following Cash and Yuste (1999), we discarded the data in such cases. Fourth, summation between branches was again overwhelmingly linear but was now more similar in form for peak and mean response measures (green circles in Figures 4C and 4D). In particular, the prominent boosting interaction seen for summation of mean responses to very strong single-shock inputs essentially disappears for high-frequency inputs.

As before, the extremes of nonlinear summation within each branch were, across the population, much larger and well separated from the very modest extreme values seen for between-branch cases The one exception to this rule, just as for the single-impulse case, was that for within-branch stimulation, mean responses rarely if ever ventured far into sublinear territory and thus could not be reliably distinguished from the population of between-branch cases.

Overall, in spite of the extremely complex response dynamics associated with high-frequency stimulation (see insets in Figures 4A and 4B), the results of the 50 Hz runs were simpler to interpret than those generated using single-shock stimuli. At the somatic recording electrode, the arithmetic of synaptic summation within a thin distal branch appeared more nonlinear, more clearly sigmoidal, and less dependent on response measure (Figures 4A and 4B). Moreover, summation between branches was remarkably close to the linear benchmark across a wide range of stimulus intensities and for both peak and mean response measures (Figures 4C and 4D). Within the limitations of the pairwise summation method, therefore, the data from our model cell are most consistent with a two-layer sum-of-sigmoidal-subunits model and are inconsistent with a linear model.

Discussion

Rules of Synaptic Integration

The pairwise summation experiments of Figures 3 and 4 were designed to distinguish between linear and nonlinear models of synaptic integration. Our results are most consistent with the model of a CA1 pyramidal cell expressed by Equation 2, in which each thin branch is an independent subunit with a sigmoidal input-output nonlinearity, and the branch-subunit outputs are combined linearly at the cell body.

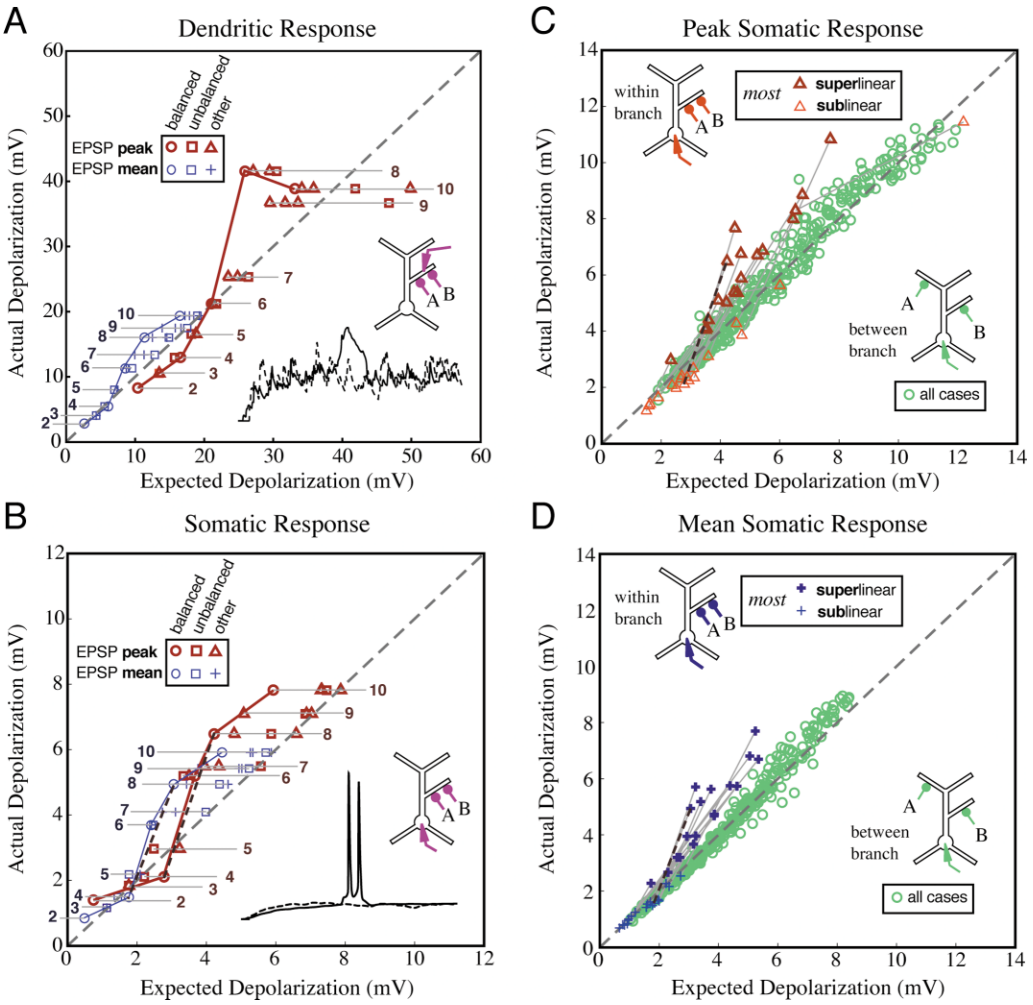

Figure 4. Repeat of Thin-Branch Summation Experiment of Figure 3, but with High-Frequency Stimulation Runs Lasting 250 ms

Each individual stimulus consisted of one to ten excitatory synapses activated by independent 50 Hz Poisson trains and one inhibitory synapse also activated by a random 50 Hz train.

(A and B) All symbols are as in Figures 3A and 3B. Insets show expected versus actual traces for one experiment, with A = B = 6 synapses.

(C and D) When combined stimulus was delivered to a single branch (within-branch condition), only one inhibitory synapse was included to maintain biophysical uniformity between runs; the expected depolarization was calculated as $r(A) + r(B) - r(i)$, where $r(i)$ is the hyperpolarizing response to a lone inhibitory synapse activated on the branch.

This conclusion is based on two main observations. First, by tracking the pattern of response summation within each dendritic branch over a wide range of input intensities, we noted a consistent progression of summation arithmetic for balanced cases strongly suggestive of a sigmoidal subunit nonlinearity. In the case of 50 Hz stimulation where the results are clearer, summation was linear for the weakest input pairs, superlinear for intermediate pairs, followed by a roll off back toward linear/sublinear summation for the strongest input pairs. Bona fide sublinear summation was never observed using 50 Hz stimulation, however, since the very strong input pairs destined to produce response saturation inevitably also triggered somatic spikes, which disqualified these data from inclusion in the scatter plot (following Cash and Yuste, 1999).

Second, by comparing summation within branches to summation between branches, we established that nonlinear interactions between inputs delivered to the same branch are not mediated by a dendrite-wide nonlinearity. Had they been, summation between branches ought to have shown a similar kind and degree of nonlinear interaction, but this was not the case. Summation between branches was remarkably linear.

Comparison of Response Measures

We compared summation arithmetic for two different response measures: mean versus peak subthreshold somatic potential. For single-impulse stimuli, different conclusions could be drawn depending on the choice of a peak versus mean response measure. For example, within-branch summation was more strongly biased to the superlinear range for mean compared to peak responses, owing largely to the contributions of voltage-dependent NMDA and Ca^{2+} channels to the late phase of the response. For related reasons, summation of mean

responses when inputs were delivered to two different branches also showed a clear bias to superlinearity, but only in the late response under the strongest input conditions. (In contrast, peak response summation was almost perfectly linear.) This suggests that a pan-dendrite boosting interaction can occur when the cell is presented with a single large pulse of excitation but that the superlinear interaction takes time to develop. The differences between peak and mean response measures mostly disappeared, however, when 50 Hz stimulation was used including inhibitory inputs. Over the 250 ms duration of the 50 Hz trials, both peak and mean summation followed a very similar sigmoidal relation.

Comparison of Single Pulse and 50 Hz Stimulation

A second goal of this study was to compare summation arithmetic for single impulse versus 50 Hz stimulation. The electrophysiological state of the postsynaptic cell is radically different under the two conditions. In one case, a cell resting at −70mV is driven by single synchronous shock delivered to a population of excitatory synapses. Locally within the dendritic branch, and at the cell body, the response to inputs of moderate intensity is most often a few tens of milliseconds in duration and straightforward—i.e., EPSP-like—in form. In contrast, a very strong shock could activate a dendritic calcium spike with Na^+ spikes riding atop, though the overall shape of the response remained single event-like. The dendritic response to 50 Hz stimulation is far more complicated, with small fast Na^+ spikelets alternating with hyperpolarization and complex calcium and NMDA-dependent depolarizations.

Given the much greater complexity of both the stimulus and response under conditions of 50 Hz stimulation, it is surprising that the laws of pairwise summation were simpler and in closer adherence to the abstract two-layer model expressed by Equation 2. In particular, from the vantage point of the soma, summation within a dendritic branch appeared to follow a simple sigmoidal relation under 50 Hz stimulation, as opposed to the weakly modulated multihumped function seen for impulse stimulation. Moreover, summation between branches was more uniformly linear and independent of response measure using 50 Hz stimuli. Neither of these outcomes could have been anticipated, nor are they easily explained based on the properties of the 21 channel types present in our model cell. For this reason, the emergent simplicity in the pattern of responses is interesting.

Methodological Issues in Pairwise Summation Experiments

The present set of modeling experiments highlights several methodological pitfalls that could lead to confusion or misinterpretation regarding the arithmetic of synaptic summation in a complex neuron.

Limitation to Paired Inputs

Experiments involving a comparison of just two inputs presented separately and together provide an inherently weak assay of a dendritic input-output nonlinearity. More powerful tests can be constructed by comparing N inputs presented separately and together where $N > 2$. Consider the hypothetical subunit function $s(x) = x^2$, where x is the total input to a subunit and s is the output. While it is true that the accelerating nonlinearity can be detected by noting that $(1 + 1)^2 > 1^2 + 1^2$, a comparable test with four inputs leads to a much larger difference between predicted and actual responses, that is, $(1 + 1 + 1 + 1)^2 >> 1^2 + 1^2 + 1^2 + 1^2$.

Input Range Limitation

The range of input magnitudes tested can influence conclusions drawn regarding synaptic summation. For example, in our model cell, the great majority of responses in single-impulse experiments were in the linear to superlinear range when predictions were 4mV or less (Figures 3C and 3D). (In this range, summation of EPSP peaks grew to an average of 132% of the linear benchmark for optimal stimuli.)

Use of Subthreshold Response Measure

Restriction of data analysis to subthreshold voltage responses at the cell body means data will be discarded when a combined stimulus leads to a somatic spike. This produces a systematic reporting bias against cases that generate the largest responses, which can arise either from very strong inputs or from weaker inputs that combine to produce unexpectedly large responses. A bias of either type can influence interpretations regarding the integrative propensities of the cell.

Poor Visibility of Distal Events

The soma provides a poor vantage point from which to view integrative events in remote dendritic branches. Powerful nonlinear effects arising from threshold crossings or saturation, which may be clearly visible at the site of synaptic input, can be attenuated to the point of ambiguity when viewed through a somatic recording electrode.

Weakness of the Scatter Plot Representation

A "predicted versus actual" scatter plot provides a poor representation of synaptic summation arithmetic. The spread in actual responses for any given prediction value—where one case might reflect superlinear summation in branch A, another linear summation in branch B, and another sublinear summation in branch C—leads the eye to see only the central tendency of the response distribution and to conclude that summation in all three branches is "linear on average." For this reason, scalar measures such as "average percent linearity" can be misleading.

Uncontrolled Stimulus Strength and Balance

Averaging of heterogeneous scatter data is even more problematic when the data set contains an uncontrolled mixture of balanced and unbalanced stimulus cases and weak versus strong stimulus cases (Figures 2A and 2C). Inclusion of unbalanced cases introduces a bias toward the hypothesis of linearity, and inclusion of more weak or more intermediate or stronger stimulus cases can introduce a bias toward the conclusion of linear or superlinear or sublinear summation, depending on the form of the subunit nonlinearity. These pitfalls can be averted and synaptic arithmetic can be more reliably characterized by tracking the responses to a wide range of inputs delivered to single identified branches (Figure 3B). Further, when the objective is to accept or reject the hypothesis that synaptic summation is linear, it is particularly important to record the maximum excursions from linearity, in either direction, on a branch-by-branch basis (Figures 3C and 3D). This leads to a clearer

picture of the arithmetic of synaptic summation than does an unannotated cloud of scatter data.

Sensitivity to Choice of Response Measure

We found that the somatic voltage peak evoked by a single synaptic impulse emphasized the very early response and correspondingly deemphasized the more powerful superlinear integrative effects due to voltage-dependent synaptic or intrinsic conductances operating on slower time scales (e.g., NMDA, persistent Na^+, and Ca^{2+} channels). On the other hand, use of the time-averaged somatic response extended the range of superlinear summation to much stronger inputs. This produced an inadvertent bias against the observation of sublinear summation, since the very strong inputs likely to produce response saturation generally also produced somatic spikes (leading to disqualification of the data).

Sensitivity to Choice of Stimulus Format

When high-frequency trains lasting hundreds of milliseconds are used as input in lieu of discrete impulses, the electrophysiological state of the cell is entirely different, with more prominent roles for Ca^{2+}, persistent Na^+, NMDA, $GABA_B$, and Ca^{2+}-dependent potassium currents. We observed three changes in the "predicted versus actual" scatter plots when 50 Hz inputs trains were used: (1) mean and peak response measures were more similar to each other, (2) both measures showed strong superlinear responses but virtually no strong sublinear responses, and (3) summation between branches was linearized, that is, the trend to superlinear summation of mean response for the strongest impulse stimuli delivered to two branches (Figure 3D) was virtually absent (Figure 4D).

In summary, the rules of synaptic arithmetic in pyramidal cells are best characterized when (1) stimulus formats go beyond single discrete excitatory impulses, (2) dual intracellular recordings include a dendritic recording electrode as close as possible to the stimulus site(s), (3) more than two inputs are applied separately and together to compare predicted versus actual responses (3 is better than 2, and so on), (4) summation is quantified using multiple response measures at the cell body, (5) responses in the 0mV to 4mV range are specifically included in the analysis, (6) separate analysis is made of cases in which somatic spikes are generated, (7) within-branch and between-branch summation results are compared head to head, (8) summation arithmetic is tracked and plotted over a range of stimulus intensities within identified branches, and (9) quantitative measures such as average percent linearity are avoided, since they lead to inappropriate cancellation of superlinear and sublinear effects.

Functional Implication: What Does a Neuron Do?

The experiments described in this paper have been designed to shed light on the information processing functions of pyramidal neurons, the principal cell type in cortical tissue. There is general agreement that pyramidal cell dendrites contain a large number and variety of voltage-dependent channels distributed nonuniformly throughout the dendritic tree, which heavily influence the cell's integrative behavior. Recent evidence also suggests that elemental synaptic conductances may vary systematically as a function of dendritic location (Magee and Cook, 2000). However, there remain quite different views as to the functional role that these dendritic and synaptic channels may play. One view is that voltage-dependent dendritic currents and scaling of synaptic conductances exist to transform the complex and physically sprawling cell into a virtual "point neuron." According to this view, dendritic nonlinearities may exist to (1) make the cell more linear, by counteracting the classical synaptic nonlinearity that arises from the summation of conductances (Bernander et al., 1994; Cash and Yuste, 1999), and in conjunction with synaptic scaling, they could (2) make the cell more functionally compact, by counteracting the distance-dependent attenuation of synaptic responses that arise from the cable properties of dendrites (Cauller and Connors, 1992; De Schutter and Bower, 1994; Magee and Cook, 2000). Both ideas emphasize the coupling of individual synapses to the cell body and the uniformity and linearity thereof.

A second view holds that the dendrites exist to create a number of independent functional compartments within which various kinds of nonlinear computations could be carried out (Koch et al., 1983; Shepherd and Brayton, 1987; Rall and Segev, 1987; Mel, 1992a, 1992b, 1993). Our results here support a particular version of this hypothesis in which the long, thin, unbranched, synapse-rich terminal dendrites may themselves act like classical neuron-like summing units, each with its own quasi-independent subunit nonlinearity. The cell body for its part, fed either directly by the basal dendrites or by the main trunk which acts as a high-efficiency conduit from the apical dendrites, sums together the dendritic subunit outflows to determine the cell's overall response. We have previously explored some of the functional implications of such a model (Mel et al., 1998; Mel, 1999; Archie and Mel, 2000; Poirazi and Mel, 2001)—see also the companion paper (Poirazi et al., 2003).

In an object as biophysically complex as a pyramidal cell, however, it is unsafe to extrapolate from the summation of subthreshold voltage responses originating in one or two dendritic branches to in vivo-like conditions involving multisite dendritic stimulation and suprathreshold somatic responses. This gap highlights a limitation of the present modeling study and of the experimental studies that have inspired it. In a companion paper (Poirazi et al., 2003), we extend our studies of synaptic integration in the same model cell to the more realistic situation in which (1) the cell is driven by dozens of high-frequency-activated excitatory synapses distributed in complex spatial patterns on many branches of the apical tree, and (2) the cell's suprathreshold response is quantified by mean firing rate.

Experimental Procedures

In the Supplemental Data (available online at http://www.neuron.org/cgi/content/full/37/6/977/DC1), we describe the construction of the pyramidal cell model and include results of several validation studies in which the model's responses are compared to experimental data.

Acknowledgments

Thanks to Gary Holt, Jeff Magee, Nelson Spruston, and Dan Johnston for useful discussions; to the anonymous reviewers for many helpful suggestions; and to Michel Migliore for help with the I_A model.

This work was funded in part by the National Science Foundation Grant No. 9734350, by the Office of Naval Research, by a Myronis Fellowship (P.P.) and by a Marie Curie Fellowship of the European Community program Quality of Life under contract number MCF-QLK6-CT-2001-51031 (P.P.).

Received: October 9, 2001
Revised: January 14, 2003

References

Archie, K.A., and Mel, B.W. (2000). An intradendritic model for computation of binocular disparity. Nat. Neurosci. *3*, 54–63.

Bernander, O., Koch, C., and Douglas, R.J. (1994). Amplification and linearization of distal synaptic input to cortical pyramidal cells. J. Neurophysiol. *72*, 2743–2753.

Cannon, R., Turner, D., Pyapali, G.K., and Wheal, H. (1998). An online archive of reconstructed hippocampal neurons. J. Neurosci. Methods *84*, 49–54.

Cash, S., and Yuste, R. (1998). Input summation by cultured pyramidal neurons is linear and position-independent. J. Neurosci. *18*, 10–15.

Cash, S., and Yuste, R. (1999). Linear summation of excitatory inputs by CA1 pyramidal neurons. Neuron *22*, 383–394.

Cauller, L.J., and Connors, B.W. (1992). Functions of very distal dendrites: Experimental and computational studies of layer I synapses on neocortical pyramidal cells. In Single Neuron Computation, T. McKenna, J. Davis, and S. Zornetzer, Eds. (Boston: Academic Press), pp. 199–229.

De Schutter, E., and Bower, J. (1994). Simulated responses of cerebellar Purkinje cells are independent of the dendritic location of granule cell synpatic inputs. Proc. Natl. Acad. Sci. USA *91*, 4736–4740.

Gillessen, T., and Alzheimer, C. (1997). Amplification of EPSPs by low Ni^{2+}- and amiloridesensitive Ca^{2+} channels in apical dendrites of rat CA1 pyramidal neurons. J. Neurophysiol. *77*, 1639–1643.

Golding, N.L., and Spruston, N. (1998). Dendritic sodium spikes are variable triggers of axonal action potentials in hippocampal CA1 pyramidal neruons. Neuron *21*, 1189–1200.

Golding, N.L., Jung, H.-Y., Mickus, T., and Spruston, N. (1999). Dendritic calcium spike initiation and repolarization are controlled by distinct potassium channel sybtypes in CA1 pyramidal neurons. J. Neurosci. *19*, 8789–8798.

Gonzalez-Burgos, G., and Barrionuevo, G. (2001). Voltage-gated sodium channels shape subthreshold EPSPs in layer 5 pyramidal neurons from rat prefrontal cortex. J. Neurophysiol. *86*, 167–184.

Häusser, M., Spruston, N., and Stuart, G.J. (2000). Diversity and dynamics of dendritic signaling. Science *290*, 739–744.

Hines, M.L., and Carnevale, N.T. (1997). The NEURON simulation environment. Neural Comput. *9*, 1179–1209.

Koch, C., Poggio, T., and Torre, V. (1983). Nonlinear interaction in a dendritic tree: Localization, timing and role of information processing. Proc. Natl. Acad. Sci. USA *80*, 2799–2802.

Lipowsky, R., Gillessen, T., and Alzheimer, C. (1996). Dendritic Na^{+} channels amplify EPSPs in hippocampal CA1 pyramidal cells. J. Neurophysiol. *76*, 2181–2191.

Magee, J.C., and Cook, E.P. (2000). Somatic EPSP amplitude is independent of synapse location in hippocampal pyramidal neurons. Nat. Neurosci. *3*, 895–903.

Magee, J., Hoffman, D., Colbert, C., and Johnston, D. (1998). Electrical and calcium signalling in dendrites of hippocampal pyramidal neurons. Annu. Rev. Physiol. *60*, 327–346.

Margulis, M., and Tang, C.-M. (1998). Temporal integration can readily switch between sublinear and supralinear summation. J. Neurophysiol. *79*, 2809–2813.

Mel, B.W. (1992a). The clusteron: Toward a simple abstraction for a complex neuron. In Advances in Neural Information Processing Systems, Volume 4, J. Moody, S. Hanson, and R. Lippmann, Eds. (San Mateo, CA: Morgan Kaufmann), pp. 3542.

Mel, B.W. (1992b). NMDA-based pattern discrimination in a modeled cortical neuron. Neural Comp. *4*, 502–516.

Mel, B.W. (1993). Synaptic integration in an excitable dendritic tree. J. Neurophysiol. *70*, 1086–1101.

Mel, B.W. (1999). Why have dendrites? A computational perspective. In Dendrites, G. Stuart, N. Spruston, and M. Hausser, Eds. (Oxford: Oxford University Press), pp. 271–289.

Mel, B.W., Ruderman, D.L., and Archie, K.A. (1998). Translation-invariant orientation tuning in visual complex cells could derive from intradendritic computations. J. Neurosci. *17*, 4325–4334.

Nettleton, J.S., and Spain, W.J. (2000). Linear to supralinear summation of AMPA-mediated EPSPs in neocortical pyramidal neurons. J. Neurophysiol. *83*, 3310–3322.

Poirazi, Y., and Mel, B.W. (2001). Impact of active dendrites and structural plasticity on the memory capacity of neural tissue. Neuron *29*, 779–796.

Poirazi, P., Brannon, T.M., and Mel, B.W. (2003). Pyramidal neuron as two-layer neural network. Neuron *37*, this issue, 989–999.

Rall, W., and Segev, I. (1987). Functional possibilities for synapses on dendrites and on dendritic spines. In Synaptic Function, G. Edelman, W. Gall, and W. Cowan, Eds. (New York: Wiley), pp. 605–636.

Reyes, A. (2001). Influence of dendritic conductances on the input-output properties of neurons. Annu. Rev. Neurosci. *24*, 653–675.

Schiller, J., Major, G., Koester, H.J., and Schiller, Y. (2000). NMDA spikes in basal dendrites of cortical pyramidal neurons. Nature *404*, 285–289.

Schwindt, P., and Crill, W. (1998). Synaptically evoked dendritic action potentials in rat neocortical pyramidal neurons. J. Neurophysiol. *79*, 2432–2446.

Shepherd, G., and Brayton, R. (1987). Logic operations are properties of computer-simulated interactions between excitable dendritic spines. J. Neurosci. *21*, 151–166.

Skydsgaard, M., and Hounsgaard, J. (1994). Spatial integration of local transmitter responses in motoneurones of the turtle spinal cord in vitro. J. Physiol. *479*, 233–246.

Urban, N.N., and Barrionuevo, G. (1998). Active summation of excitatory postsynaptic potentials in hippocampal CA3 pyramidal neurons. Proc. Natl. Acad. Sci. USA *95*, 11450–11455.

Urban, N.N., Henze, D.A., and Barrionuevo, G. (1998). Amplification of perforant-path EPSPs in CA3 pyramidal cells by LVA calcium and sodium channels. J. Neurophysiol. *80*, 1558–1561.

Wei, D.S., Mei, Y.A., Bagal, A., Kao, J.P., Thompson, S.M., and Tang, C.M. (2001). Compartmentalized and binary behavior of terminal dendrites in hippocampal pyramidal neurons. Science *293*, 2272–2275.

Wessel, R., Kristan, W.B.J., and Kleinfeld, D. (1999). Supralinear summation of synaptic inputs by an invertebrate neuron: dendritic grain is mediated by an inward rectifier K^{+} current. J. Neurosci. *19*, 5875–5888.